

## Supporting Information

### **Oxygen Vacancy Enriched Hollow Cobaltosic Oxide Frames with Ultrathin Walls for Efficient Energy Storage and Biosensing**

Li Hua,<sup>a</sup> Zengyu Hui,<sup>a</sup> Yue Sun,<sup>a</sup> Xi Zhao,<sup>a</sup> Hai Xu,<sup>a</sup> Yujiao Gong,<sup>a</sup> Ruyi Chen,<sup>a</sup> Chenyang Yu,<sup>a</sup> Jinyuan Zhou,<sup>c</sup> Gengzhi Sun<sup>\*a</sup> and Wei Huang<sup>ab</sup>

<sup>a</sup>Key Laboratory of Flexible Electronics (KLOFE) & Institute of Advanced Materials (IAM), Nanjing Tech University (NanjingTech), 30 South Puzhu Road, Nanjing 211816, P. R. China. E-mail: [iamgzsun@njtech.edu.cn](mailto:iamgzsun@njtech.edu.cn)

<sup>b</sup>Shaanxi Institute of Flexible Electronics (SIFE), Northwestern Polytechnical University, 127 West Youyi Road, Xi'an 710072, P. R. China.

<sup>c</sup>School of Physical Science and Technology, Lanzhou University, 222 South Tianshui Road, Lanzhou 730000, P. R. China.

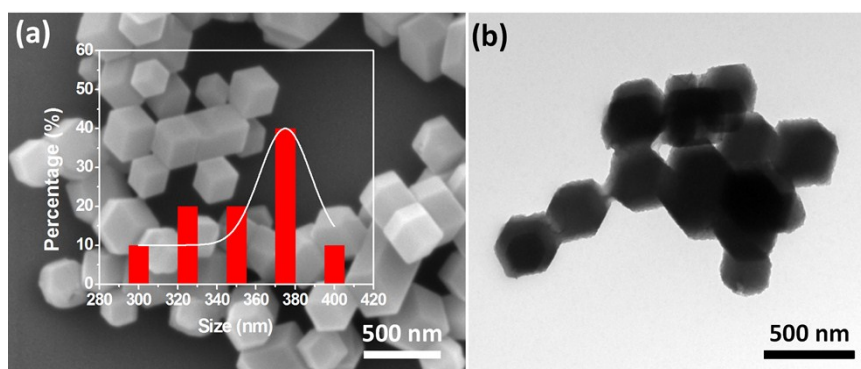


**Fig. S1** Typical SEM (a) and TEM (b) images of Co-MOF (ZIF-67) rhombic dodecahedron. Inset in (a) is the size distribution of ZIF-67.

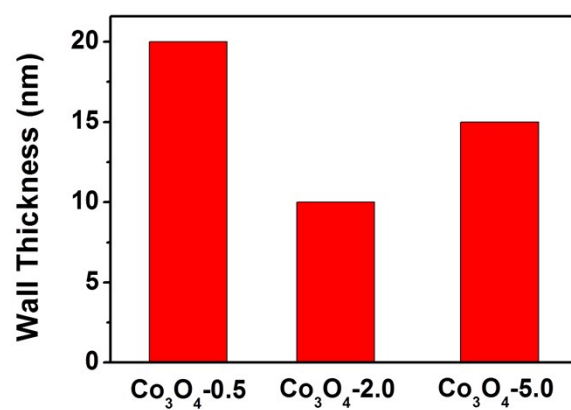


**Fig. S2** The wall thickness of  $\text{Co}_3\text{O}_4\text{-0.5}$ ,  $\text{Co}_3\text{O}_4\text{-2.0}$  and  $\text{Co}_3\text{O}_4\text{-5.0}$ .

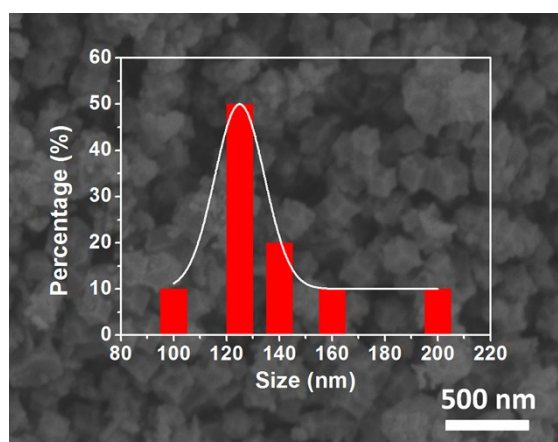


**Fig. S3** Typical SEM image of Co<sub>3</sub>O<sub>4</sub>-10.0 obtained by calcination of ZIF-67 in air at 300 °C with the ramping rate of 10.0 °C min<sup>-1</sup>. Inset is the size distribution of Co<sub>3</sub>O<sub>4</sub>-10.0.

**Table S1** Summary of O 1s XPS spectra of Co<sub>3</sub>O<sub>4</sub>-0.5, Co<sub>3</sub>O<sub>4</sub>-2.0 and Co<sub>3</sub>O<sub>4</sub>-5.0.

Co <sub>3</sub> O <sub>4</sub> samples		O <sub>L</sub> (Co-O)	O <sub>V</sub> (vacancy)
Co <sub>3</sub> O <sub>4</sub> -0.5	binding energy (eV)	530.0	530.9
	relative percentage (%)	68.0	32.0
Co <sub>3</sub> O <sub>4</sub> -2.0	binding energy (eV)	530.2	531.0
	relative percentage (%)	56.2	43.8
Co <sub>3</sub> O <sub>4</sub> -5.0	binding energy (eV)	530.0	530.9
	relative percentage (%)	76.8	23.2

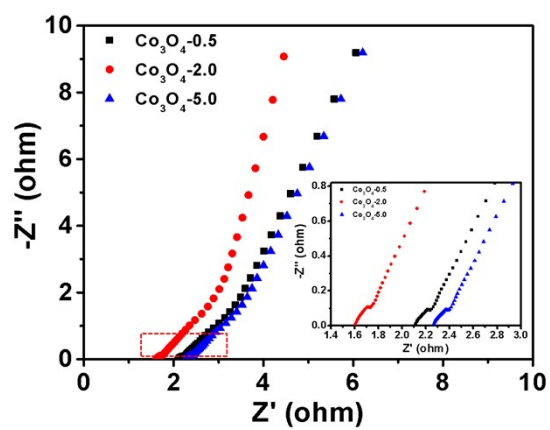


**Fig. S4** Nyquist plots of the EIS of  $\text{Co}_3\text{O}_4-0.5$ ,  $\text{Co}_3\text{O}_4-2.0$  and  $\text{Co}_3\text{O}_4-5.0$ .

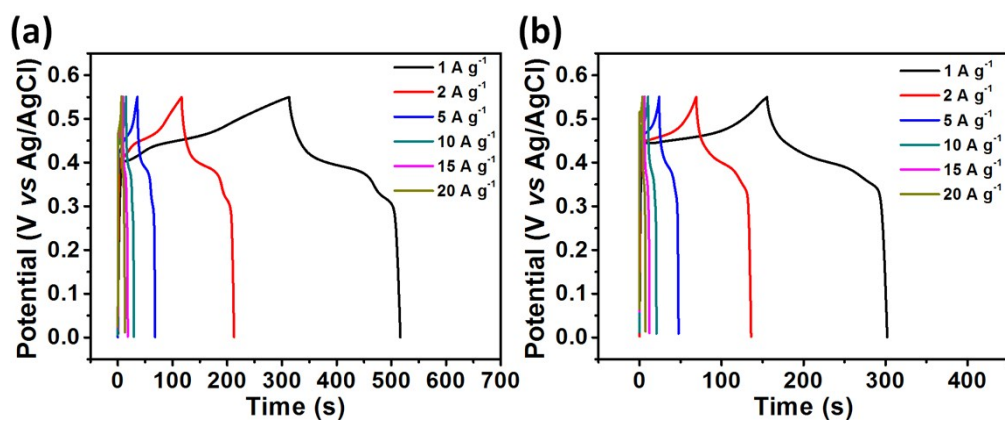


**Fig. S5** Charge-discharge curves of (a)  $\text{Co}_3\text{O}_4\text{-0.5}$  and (b)  $\text{Co}_3\text{O}_4\text{-5.0}$  measured at different current densities.

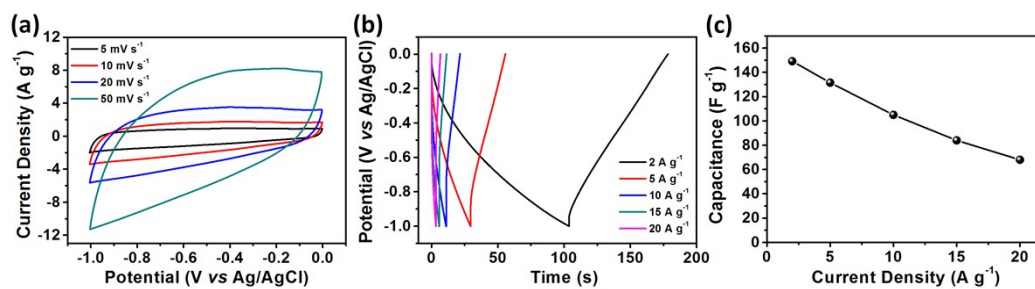


**Fig. S6** (a) Cyclic voltammogram curves of holey graphene at different scan rates ranging from 5 to 50 mV s<sup>-1</sup>. (b) Charge-discharge curves and (c) the corresponding specific capacitance of holey graphene measured at different current densities.



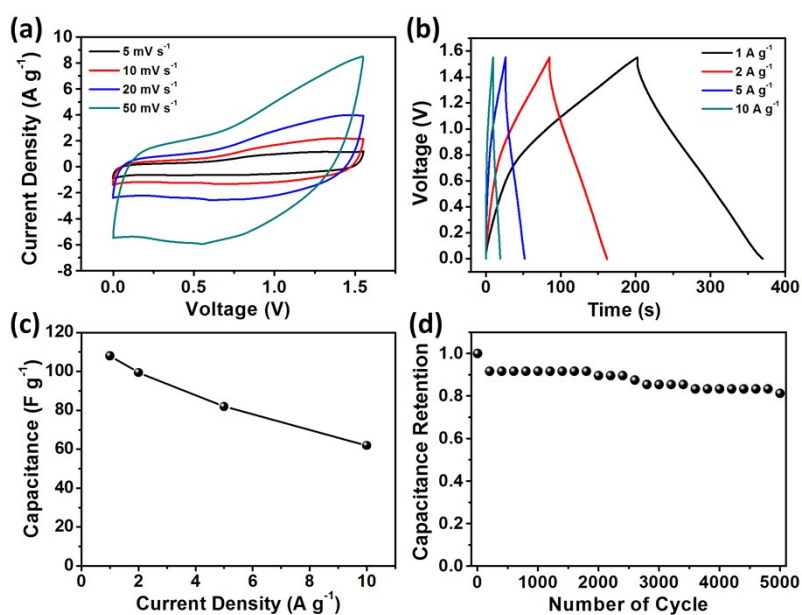


**Fig. S7** (a) The CV curves of the hybrid supercapacitors made of  $\text{Co}_3\text{O}_4\text{-2.0}$  and holey graphene as the positive and negative respectively at different scan rates ranging from 5 to 50  $\text{mV s}^{-1}$ . (b) Charge-discharge curves and (c) the corresponding specific capacitance of the hybrid supercapacitor at different current densities. (d) Cycling performance of the hybrid supercapacitor at the current density of 10  $\text{A g}^{-1}$ .